



UNIVERSITY OF LEEDS

This is a repository copy of *CFD Simulation of Single- and Two-Phase Natural Convection in the Context of External Reactor Vessel Cooling*.

White Rose Research Online URL for this paper:

<http://eprints.whiterose.ac.uk/128024/>

Version: Accepted Version

Proceedings Paper:

Colombo, M and Fairweather, M (2017) CFD Simulation of Single- and Two-Phase Natural Convection in the Context of External Reactor Vessel Cooling. In: Proceedings of the 17th International Topical Meeting on Nuclear Reactor Thermal Hydraulics. 17th International Topical Meeting on Nuclear Reactor Thermal Hydraulics (NURETH-17), 03-08 Sep 2017, Xi'an, Shaanxi, China. .

This is an author produced version of a paper published in the Proceedings of the 17th International Topical Meeting on Nuclear Reactor Thermal Hydraulics. All rights reserved.

Reuse

Unless indicated otherwise, fulltext items are protected by copyright with all rights reserved. The copyright exception in section 29 of the Copyright, Designs and Patents Act 1988 allows the making of a single copy solely for the purpose of non-commercial research or private study within the limits of fair dealing. The publisher or other rights-holder may allow further reproduction and re-use of this version - refer to the White Rose Research Online record for this item. Where records identify the publisher as the copyright holder, users can verify any specific terms of use on the publisher's website.

Takedown

If you consider content in White Rose Research Online to be in breach of UK law, please notify us by emailing eprints@whiterose.ac.uk including the URL of the record and the reason for the withdrawal request.

CFD SIMULATION OF SINGLE- AND TWO-PHASE NATURAL CONVECTION IN THE CONTEXT OF EXTERNAL REACTOR VESSEL COOLING

Marco Colombo and Michael Fairweather

School of Chemical and Process Engineering, University of Leeds, Leeds LS2 9JT,
United Kingdom

M.Colombo@leeds.ac.uk; M.Fairweather@leeds.ac.uk

ABSTRACT

In recent decades, and with renewed importance after the events in Fukushima, the nuclear community has focused on the opportunity to rely on passive safety and, after plant shutdown, to ensure that reactor cooling can be safely guaranteed by natural processes, at least for a sufficient time before any active power intervention is needed. Buoyancy-driven flows and natural convection provide an efficient and potentially highly reliable and inexpensive heat transfer mechanism but, at the same time, these are rather complex flows because of the strong two-way coupling between the velocity and thermal fields, and the interaction between buoyancy and turbulence. In view of this, numerical tools able to predict these flows with accuracy and confidence are necessary to support the informed design and the safety assessment of present and future nuclear power plants. This paper is focused on research ongoing at the University of Leeds on the development of computational fluid dynamic tools to predict buoyancy-driven flows, of particular relevance to external reactor vessel cooling (ERVC). In ERVC, the aim is to retain the melted corium inside the reactor vessel, which is cooled from the outside by natural convection in the flooded reactor cavity where boiling is expected to occur on the outer vessel wall. The work starts by considering single-phase flow in a square buoyant cavity that is used to assess and improve the accuracy of available Reynolds-averaged Navier-Stokes (RANS) models, some of which, through the turbulence models embedded within them, are known to have shortcomings in predicting natural convection. In the same geometry, the superior accuracy of the large eddy simulation technique, the results from which may underpin further development of RANS approaches, is demonstrated. A two-fluid Eulerian-Eulerian model including boiling at the wall, which will be required to predict the whole ERVC phenomena, is also preliminary tested in the final part of the paper. Overall, encouraging results are found and weaknesses of the available modelling techniques and areas for future development are identified.

KEYWORDS

Computational fluid dynamics, natural convection, buoyancy-driven flows, external reactor vessel cooling

1. INTRODUCTION

Natural convection arises in a fluid every time a temperature gradient induces a density gradient. The cooler and heavier fluid naturally moves towards the bottom of the system and the hotter and lighter fluid towards the top, promoting natural circulation and different types of buoyancy-driven and mixing phenomena. In multiphase flows, these phenomena are also generated by gradients in the phase distribution, provided that the phases have a different density. Natural convection is regarded as an efficient, cost-effective and reliable heat transfer mechanism that relies solely on naturally occurring phenomena, possibly lasting indefinitely without interruption, and does not require any active power or moving parts. In view of this, natural convection is used in numerous heat transfer, air ventilation and thermal storage applications in almost all engineering sectors. The nuclear industry recognized the benefits of natural convection some decades ago and many modern reactor designs, some of which are

already in operation or currently under construction, rely on passive cooling in some or all of their safety systems, or even during normal operation [1]. In the aftermath of recent events in Fukushima, the use of passive safety has significantly increased and it is now regarded as necessary to be able to guarantee, after plant shutdown or a reactor fault, a certain grace time during which passive cooling of the plant is ensured and before any active powered intervention is needed [2].

Despite their potential simplicity and reliability, natural convective and buoyancy-driven flows are complex since the thermal field and the velocity field are strongly coupled. Flow instabilities are often a serious risk in these flows [3], and phenomena such as thermal stratification can prevent a system removing the amount of heat required by design [4]. In addition, strong interactions occur between buoyancy forces and the turbulence field that make computation of these flows challenging [5, 6]. Depending on the geometry of the system, the body force field can increase or suppress turbulence and commonly used models, such as high-Reynolds number wall treatments, cease to be valid in natural convection boundary layers, where the velocity does not follow the universal log-low in the near-wall region [7]. Therefore, the availability of accurate numerical tools becomes an essential prerequisite to predicting these flows with confidence and to guaranteeing that design and engineering limits, which safeguard the safety and the integrity of the reactor, are always achieved.

Many recent reactor designs rely on external reactor vessel cooling (ERVC) and in-vessel retention of the melted corium to mitigate and manage severe accident scenarios that involve the melting of the fuel rods [1, 8]. In this scenario, heat is passively removed by natural convection in the flooded reactor cavity and boiling is expected to occur on the outer vessel wall. Therefore, a limit on the cooling capability of the system will be imposed by the critical heat flux (CHF) [8, 9]. To predict ERVC as well as other buoyancy-driven phenomena, a research programme is ongoing at the University of Leeds within the framework of the UK-India Civil Nuclear Collaboration, focused on the use of computational fluid dynamic (CFD) approaches. Despite numerous experimental studies [8, 10, 11], CFD has been rarely applied to these flows. CFD has the capability, with respect to more traditional one-dimensional approaches currently used in the nuclear industry, to account fully for three-dimensional effects across the different length scales of interest, and to predict with detail temperatures and flow distributions, as well as higher thermal load regions and hot spots.

Krepper et al. [12] applied a laminar single-phase CFD model based on the Boussinesq approximation to study and improve the prediction of thermal stratification for a condenser submerged in a pool. Gandhi et al. [13, 14] studied thermal stratification for a vertical rod submerged in a cylindrical [13] and a rectangular [14] pool. Boiling at the wall was observed in their experiments and, therefore, these were predicted with a mixture Eulerian model coupled with a $k-\omega$ turbulence model. Minocha et al. [4] also predicted the single-phase flow in an isolation condenser pool and compared the performance of different turbulence models.

In this paper, the development of a CFD model in the STAR-CCM+ code [15] for the prediction of natural convection in single-phase turbulent flows, and a preliminary extension to two-phase boiling flow conditions, are presented. Single-phase simulations of a square buoyant cavity are presented and different RANS-based approaches are tested. More specifically, the performance of the turbulence model is evaluated in detail and alternative modelling of the near-wall region and the turbulent components of the heat flux are evaluated for a square buoyant cavity flow. Buoyant cavities have been extensively studied in the literature, since the geometry is relatively simple, but at the same time, representative of many practical applications [7, 16, 17]. Therefore, they are a good test case for CFD models, with accurate experimental measurements as well as results obtained with direct numerical simulation and large eddy simulation (LES) approaches [18, 19] being available. In view of this, results derived from an LES implemented in OpenFOAM [20] are also compared against the experimental data. Geometries such as those of buoyant cavities in fact require a relatively low computational effort that allows the use of LES

which, given the high level of detail it gives, can provide the additional knowledge required to underpin further developments of RANS models. In addition, many natural convective flows of interest in nuclear reactors, including ERVC, involve some degree of boiling. With this in mind, in the final part of the paper a two-fluid Eulerian-Eulerian boiling model is preliminary tested against an experiment on a vertical heated rod submerged in a cylindrical water pool [13]. The performance and limitations of the available models are discussed and an outlook on future developments provided.

2. EXPERIMENTAL WORK

The experimental measurements obtained in a square buoyant cavity by Ampofo and Karayannidis [16] were used to test the single-phase models. The air-filled cavity was 0.75×0.75 m in height and width and 1.5 m deep. A two-dimensional buoyancy-driven recirculating flow having a Rayleigh number $Ra = 1.58 \times 10^9$ was generated by heating the left side wall at 50°C and cooling the right side wall to 10°C . Simultaneous measurements of temperature and velocity were obtained using E-type thermocouples and a laser-Doppler anemometry technique. Profiles of temperature, velocity, temperature fluctuations, Reynolds stresses and turbulent heat fluxes were measured at the half-height in the cavity. In view of the accuracy of the measurements, these data provide a good benchmark database for the validation of CFD models and have been used in the past for validation of both RANS [7] and LES approaches [19].

Gandhi et al. [13] measured temperature and velocity fields around a vertical rod submerged in a cylindrical water pool to study thermal stratification. The water tank was 0.3 m in diameter and 0.45 m in height, and was filled with water up to a height of 0.3 m. The outside diameter of the heated rod in the centre was 0.02 m. Velocity and temperature measurements at different locations were obtained using particle-image velocimetry and K-type thermocouples. For this work, we selected the experiment at a Rayleigh number of 1.14×10^{11} , where the heated rod was maintained at 140°C and subcooled boiling was observed on the outer wall of the rod.

3. CFD MODELS

The RANS model solves the incompressible, Reynolds-averaged continuity, momentum and energy conservation equations. Buoyancy is accounted for in the gravitational term of the momentum equations only, adopting the Boussinesq approximation, which is acceptable provided that changes in temperature T and density ρ are limited:

$$\rho = \rho_0(1 - \beta(T - T_0)) \quad (1)$$

where ρ_0 and T_0 are the reference density and temperature and β is the thermal expansion coefficient:

$$\beta = -\frac{1}{\rho_0} \frac{\partial \rho}{\partial T} \quad (2)$$

In the LES, the filtered, low-Mach number weakly compressible formulation of the Navier-Stokes equations was solved, together with the energy conservation equation [19]. In LES computations air, which fills the square cavity, is treated as a perfect gas.

3.1. Turbulence Modelling

In the RANS simulations, turbulence in the flow is solved with the standard $k-\varepsilon$ model [21], where the production of turbulence due to buoyancy is evaluated as:

$$G_b = \beta \frac{\mu_t}{\sigma_t} \frac{\partial T}{\partial x_i} g_i \quad (3)$$

Here, g is gravitational acceleration, μ_t the turbulent viscosity and σ_t the turbulent Prandtl number, fixed at 0.9. In the near-wall region, two wall-treatments are used and compared. The two-layer formulation, in the version proposed by Xu et al. [22] for natural convective flows, solves a one-equation model for the turbulence kinetic energy k , but prescribes algebraically the turbulence energy dissipation rate in the first computational cell near the wall using $\varepsilon = k^{3/2} / l_\varepsilon$. The length scale l_ε and the turbulent viscosity ratio are obtained from:

$$l_\varepsilon = \frac{8.8y}{1 + 10/y_v^* + 0.0515y_v^*} \quad (4)$$

$$\frac{\mu_t}{\mu} = \frac{0.544y}{1 + 50250y_v^{*1.65}} \quad (5)$$

In the previous equations, y is the normal distance from the nearest wall and y_v^* is a function of the wall normal stress \overline{vv} , modelled as a function of the dimensionless wall distance $y^* = yk^{0.5} / v$, where v is the kinematic viscosity [22]. In the low-Reynolds number $k-\varepsilon$ model [23], the additional production term G' and the dumping function f_2 are added to the turbulence energy dissipation rate equation [15]:

$$G' = Df_2 \left(G_k + 2\mu \frac{k}{y^2} \right) e^{(-Ey^{*2})} \quad (6)$$

$$f_2 = 1 - Ce^{Re_t^2} \quad (7)$$

In Eqs. (6) and (7), $Re_t = k^2 / \varepsilon v$, G_k is the turbulence kinetic energy production rate, $C = 0.3$, $D = 1$ and $E = 0.00375$. In the two-layer formulation, the turbulent heat fluxes are modelled extending the eddy-viscosity approach:

$$\overline{u_i \theta} = \frac{\nu_t}{\sigma_t} \frac{\partial T}{\partial x_i} \quad (8)$$

In Eq. (8), u_i are the components of the turbulent velocity fluctuations, θ is the temperature fluctuation and ν_t the turbulent kinematic viscosity. In contrast, the low-Reynolds turbulence model is coupled with the algebraic heat flux model from Kenjeres et al. [24]:

$$\overline{u_i \theta} = -C_\theta \tau \left(\zeta \overline{u_i u_j} \frac{\partial T}{\partial x_j} + \xi \overline{u_i \theta} \frac{\partial U_i}{\partial x_j} + \eta \beta g_i \overline{\theta^2} \right) + C_{\theta 1} a_{ij} \overline{u_j \theta} \quad (9)$$

Here, τ is the turbulence timescale and a_{ij} the anisotropy tensor. In addition, $C_\theta = 0.12$, $C_{\theta 1} = 1.5$, $\zeta = 1$, $\xi = 0.6$ and $\eta = 0.6$ [15]. The temperature variance $\overline{\theta^2}$ is computed by solving an additional transport equation [24]. When Eq. (9) is used, the buoyancy production of turbulence is calculated from:

$$G_b = \rho \beta g_i \overline{u_i \theta} \quad (10)$$

In the LES, the one-equation sub-grid eddy viscosity model of Yoshizawa [25] is used.

3.2. Boiling Model

An Eulerian-Eulerian, two-fluid boiling model that solves a set of mass, momentum and energy conservation equations for each phase is used in two-phase conditions. Because of averaging, closure models are included for mass, momentum and energy transfer at the interphase. In the continuous phase, the Boussinesq approximation from Eq. (1) is included to account for buoyancy effects in the liquid. Turbulence is solved in the continuous phase only with a multiphase formulation of the standard k - ε model [15] and turbulent heat fluxes are modelled following Eq. (8). Heat flux from the wall, following the Rensselaer Polytechnic Institute (RPI) heat flux partitioning approach [26], is partitioned between convection to the single-phase liquid, evaporation and quenching:

$$q_w = (q_c + q_q + q_{ev}) \quad (11)$$

The evaporative contribution to the heat flux q_{ev} is equal to:

$$q_{ev} = Nf \left(\frac{\pi d_w^3}{6} \right) \rho_v h_{lv} \quad (12)$$

In the previous equation, the active nucleation site density N , representing the number of nucleation sites per unit area, is calculated from Hibiki and Ishii [27], the bubble departure diameter d_w from Kocamustafaogullari [28] and the bubble departure frequency f from Cole [29]. The average bubble diameter in the flow is related to the local subcooling with the correlation from Kurul and Podowski [26] and evaporation/condensation in the bulk is evaluated using the Ranz and Marshall correlation [30].

3.3. Numerical Implementation

Single-phase RANS calculations were made using the STAR-CCM+ code [15]. A two-dimensional geometry was employed and simulations were run in time until steady-state conditions were reached. Simulations were considered converged when residuals dropped under 10^{-5} . The fluid was initially at rest at 30°C and the no-slip condition was imposed at the wall. Temperatures were fixed at 50°C and 10°C on the left and right walls, respectively, and the temperature profiles measured in the experiments were imposed at the upper and lower walls. The fluid had a Prandtl number $Pr = 0.71$ and the thermal expansion coefficient was fixed at $\beta = 0.00327$, derived from the Rayleigh number of 1.58×10^9 provided in [16]. A sensitivity study demonstrated that grid independence of the solutions was achieved with a 60×50 elements grid, with the first grid point at a non-dimensional distance from the wall of around 1, required for the low-Reynolds number wall treatment.

Single-phase LES simulations were made with the buoyantPimpleFoam solver from the OpenFOAM platform [20], using a cubic section of the geometry of 0.75 m depth and periodic boundaries. Boundary and initial conditions as well as fluid properties were maintained from the previous RANS simulations. A second-order implicit scheme was used for time and a central difference scheme for spatial discretization. A mesh of $128 \times 128 \times 128$ elements provided sufficient grid resolution, as found in [19]. Convergence criterion was maintained at 10^{-5} for all variables and averaging was started after 150 s of simulation, necessary for the flow to reach statistically stable conditions.

Two-phase boiling simulations were made using the STAR-CCM+ code [15]. A three-dimensional, 45 degree radial section of the geometry was built and symmetry boundary conditions were applied at the two ends. No-slip boundary conditions were imposed on the walls of the tank and the heated rod, which was kept at an imposed temperature of 140° C. On the upper free-surface, a free-slip boundary condition was applied to the liquid, which, therefore, did not leave the volume but flowed in the radial direction

towards the outside of the tank. At the same time, the boundary condition should allow any vapour to escape from the upper surface. It is anticipated here, however, that due to the very low amount of vapour generated in the case studied, it was not necessary to account for vapour leaving the volume. The simulation was run for a total of 200 s, starting from fluid initially at rest at 27°C. The fluid had a thermal expansion coefficient $\beta = 0.00068$ and a Rayleigh number $Ra = 5.9 \times 10^{11}$, equal to those values provided in [19] for the specific experiment selected. Simulations were considered converged when residuals were again lower than 10^{-5} and a sensitivity study assured that grid independent solutions were obtained, with the first grid point at a sufficient distance from the wall for a high-Reynolds wall treatment to be used.

4. RESULTS AND DISCUSSION

4.1. Single-phase RANS

A first comparison between experimental results and RANS CFD predictions is provided in Figure 1, where symbols identify experimental data and lines numerical results. The abscissa represents the horizontal position normalized by the cavity length L , and the subscript x identifies the horizontal direction and y the vertical direction. Values of all the variables have been made non-dimensional using the buoyancy velocity $V_0 = (g\theta L\Delta T)^{0.5}$ and the temperature difference ΔT . Experiments provide a picture of the flow features. Warmer fluid near the left wall has a lower density and flows upward towards the top wall, travels near the top wall across the cavity and it is cooled flowing downward in the region of the right wall. Gradients, and therefore energy and momentum transfer, are concentrated in the boundary layers very close to the walls whereas, in most of the cavity, uniform temperature and velocity profiles are found (Figure 1(a) and Figure 1(b)). A large recirculation structure is formed, with turbulent flow confined near the walls and an almost laminar flow found in the centre of the cavity (Figure 1(b)). In [16] it is stated that the boundary layers grow along the vertical walls and turbulence increases after the flow is found to be almost laminar at the bottom of the left and top of the right walls. The turbulence structure is not isotropic, and turbulent fluctuations in the vertical direction almost double those in the horizontal direction (Figure 1(c)). In a similar way, the turbulent heat flux is almost an order of magnitude higher in the vertical direction (Figure 1(e) and Figure 1(f)).

The two-layer model predicts, as expected, a near-isotropic turbulence structure and the r.m.s. profiles are mid-way between measurements in the vertical and horizontal directions (Figure 1(c)). The turbulent boundary layers are slightly more extended with respect to the experiments and zero turbulence is found in the centre of the cavity. In Figure 1(d) the Reynolds shear stress is well predicted, the only difference with experiment being again the slightly higher extension towards the centre of the cavity which translates into a slightly thicker velocity boundary layer. The velocity peak itself is, however, well predicted (Figure 1(b)). The model is not able to reproduce the structure of the turbulent heat transfer at all (Figure 1(e) and Figure 1(f)) because, following Eq. (8), the turbulent heat flux is assumed to be aligned with the temperature gradient. Instead, the experiments show a turbulent heat flux much higher in the vertical direction, even if the dominant temperature gradient is in the horizontal direction. Therefore, a model such as Eq. (8) is not able to reproduce the present natural convection boundary layer. Even so, the temperature profile in Figure 1(a) is well predicted, probably because conduction is still dominant in the cavity.

Preliminary simulations with a low-Reynolds number turbulence model showed an excessive amount of turbulence and turbulent heat flux that often prevented convergence being reached. Therefore, a previous and slightly simpler formulation was introduced for the turbulent heat fluxes [31]:

$$\overline{u_i \theta} = -C_\theta \tau \left(\overline{u_i u_j} \frac{\partial T}{\partial x_j} + \xi \overline{u_j \theta} \frac{\partial U_i}{\partial x_j} + \eta \beta g_i \overline{\theta^2} \right) \quad (13)$$

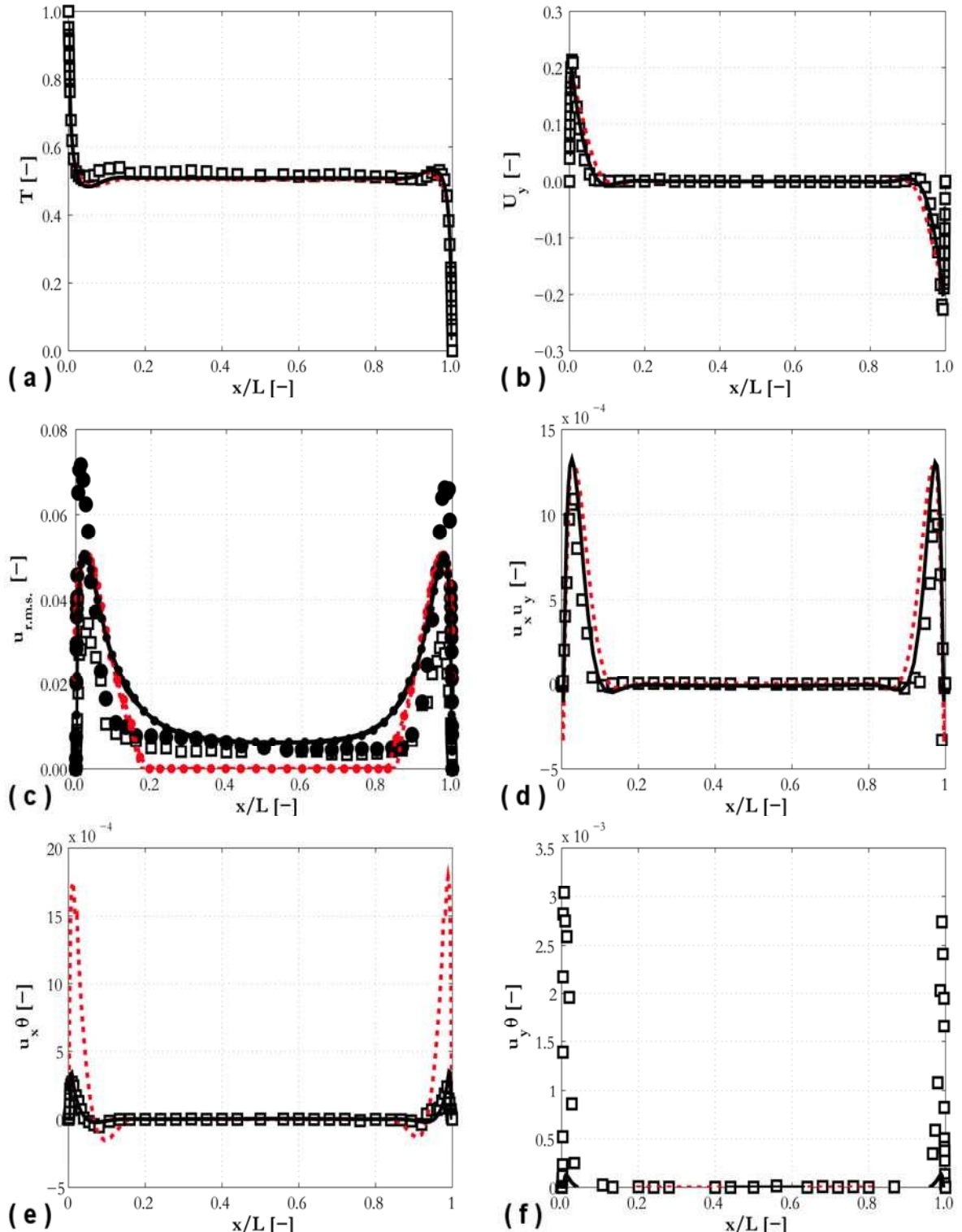


Figure 1. Profiles at half-height in the cavity of temperature (a), vertical velocity (b), r.m.s. of the velocity fluctuations (c), Reynolds shear stress (d), horizontal (e) and vertical (f) turbulent heat flux compared against experiments. (—) low-Re $k-\varepsilon$ with Eq. (13); (---) two-layer $k-\varepsilon$. In (c), squares and lines are used for horizontal r.m.s. and circles, and lines with circles, for vertical r.m.s.

With respect to Eq. (9), the last term of the anisotropy tensor is neglected, but this can be expected to have no influence in our case because, using the k - ε model, a near-isotropic turbulence field is predicted. In view of the still very high amount of turbulence generated, the contribution of Eq. (13) was reduced by changing the value of C_θ . Results with a progressively lower value of C_θ are shown in Figure 2. The plots show the predictions of flow near the left wall region of the cavity only. The best results are obtained at $C_\theta = 0.0125$, for which the Reynolds shear stress, horizontal turbulent heat flux and temperature fluctuations are well predicted. Comparison with the two-layer model results in Figure 1 show that the velocity profile is slightly improved and well predicted (Figure 1(b)), as is the turbulence in the centre of the cavity (Figure 1(c)). Although the horizontal turbulent heat flux is well predicted and greatly improved with respect to the two-layer model (Figure 1(e)), the vertical component remains significantly under predicted in Figure 1(f). Therefore, the algebraic heat flux model, coupled to a k - ε model, is not able to entirely reproduce the turbulent heat transfer in this flow.

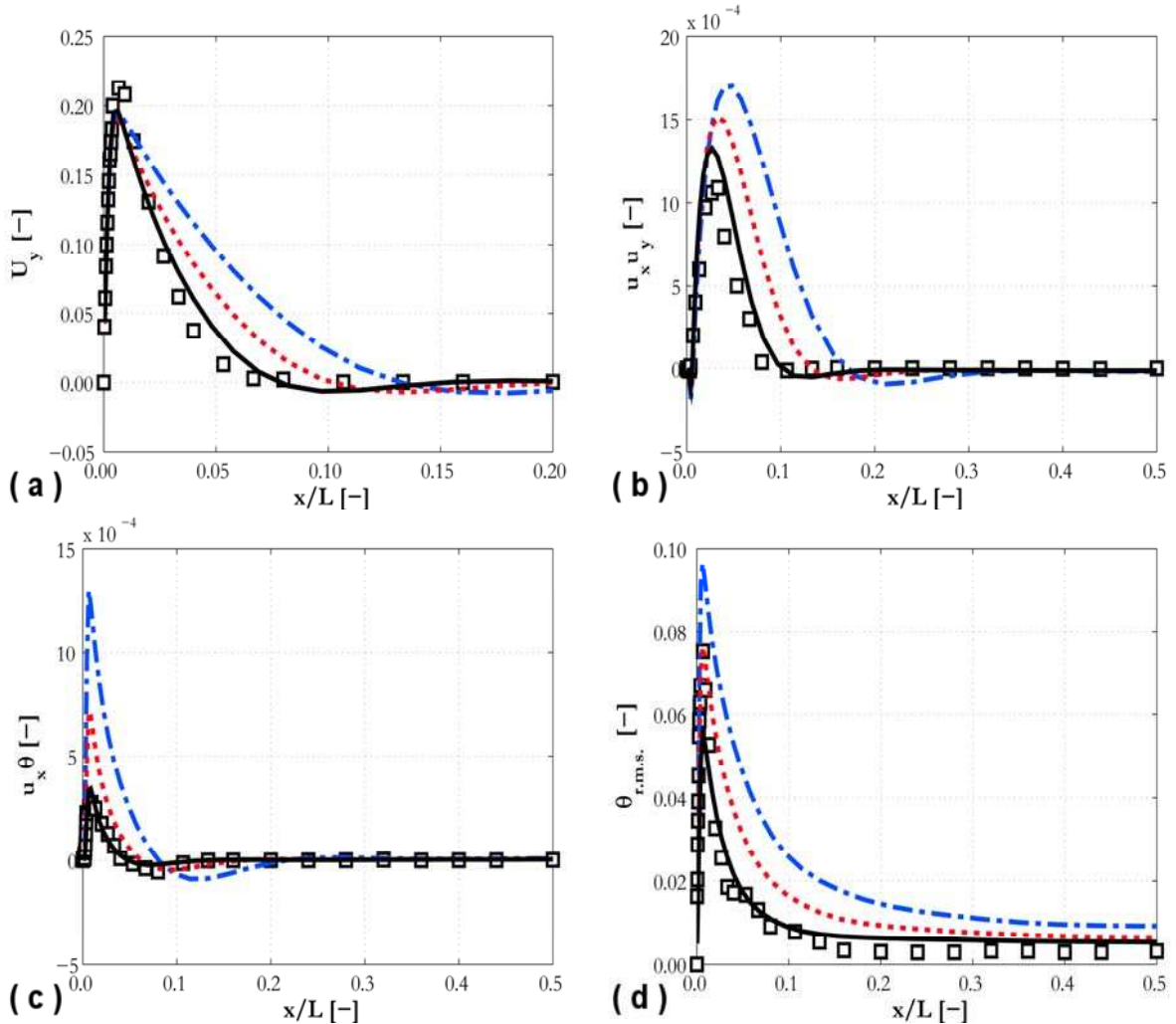


Figure 2. Profiles in the left side and at half-height in the cavity of vertical velocity (a), Reynolds shear stress (b), horizontal turbulent heat flux (c) and temperature fluctuations (d) compared against experiments. C_θ equal to 0.05 (—), 0.025 (---) and 0.0125 (—).

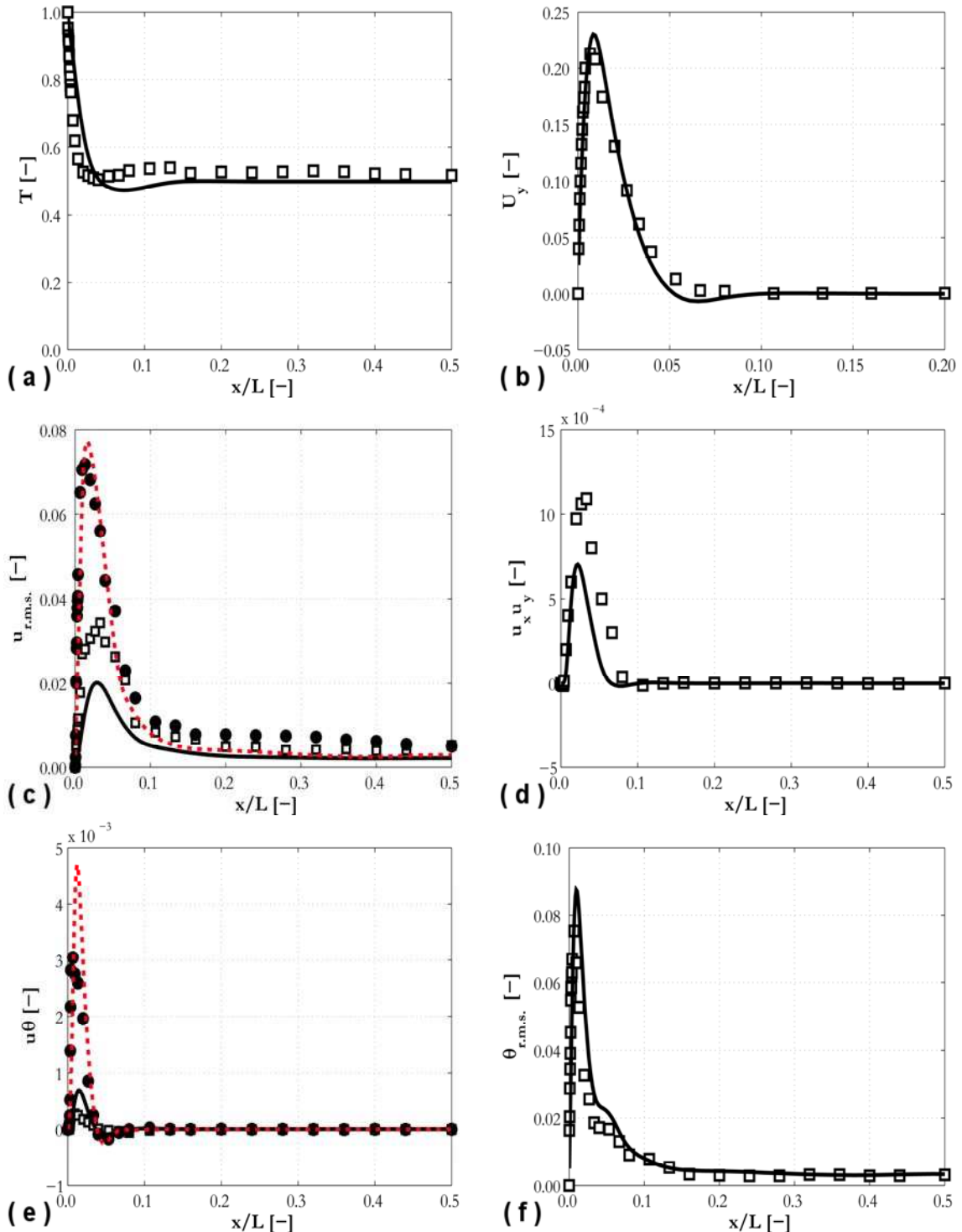


Figure 3. Profiles in the left side and at half-height in the cavity of temperature (a), vertical velocity (b), r.m.s. of the velocity fluctuations (c), Reynolds shear stress (d), horizontal and vertical turbulent heat fluxes (e) and temperature fluctuations (f) from LES compared against experiments. In (c) and (e), squares and continuous line are used for horizontal direction and circles and dotted lines for vertical.

4.2. Single-phase LES

Figure 3 presents results from the LES that are compared against the same experiment. Average temperature and velocity profiles (Figure 3(a) and Figure 3(b)) remain well predicted, and a significant improvement with respect to the two-equation eddy-viscosity models is found for the turbulence structure and the turbulent heat transfer. Anisotropy of the turbulence field is well-reproduced in Figure 3(c), although peaks in the r.m.s. of the horizontal velocity fluctuations and in the Reynolds shear stress (Figure 3(d)) are under predicted. Temperature fluctuations in Figure 3(f) are in agreement with experiment as well as the structure of the turbulent heat fluxes in Figure 3(e). The LES also correctly predicts the turbulent heat flux to be higher than the horizontal heat flux, although the peaks are over predicted for both. Similar discrepancies in horizontal r.m.s. and turbulent heat flux peaks were also reported in a previous study [19]. Clearly, the higher level of accuracy achievable with LES allows a significant improvement in the predictions with respect to the RANS models.

4.3. Two-phase simulations

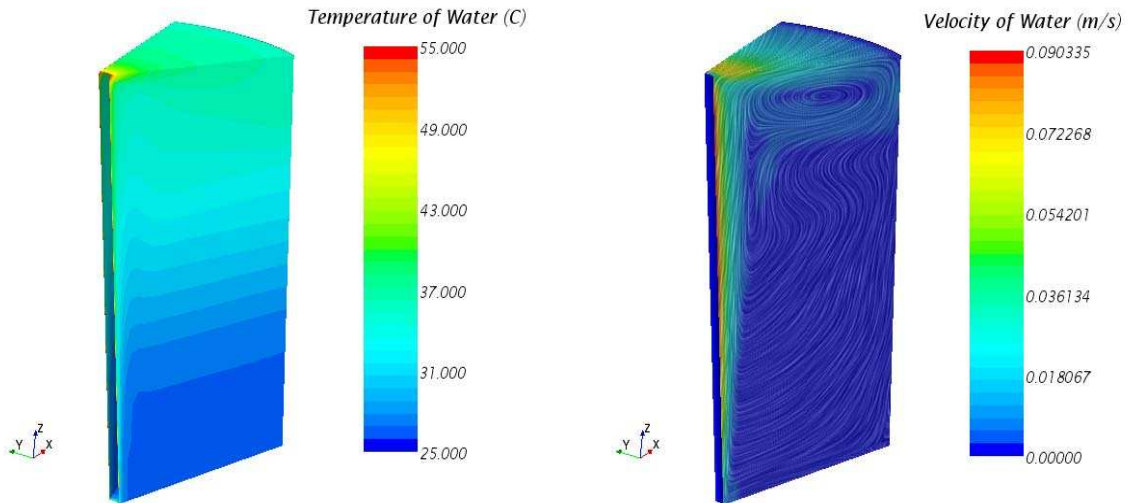


Figure 4. Water temperature and velocity fields in the water tank.

An experiment from [13] was finally predicted with the two-fluid boiling model and some preliminary results are presented in this section. As soon as the simulation is started, water is heated by the central rod and flows upwards to be replaced by cooler water coming from the bottom of the tank. When water reaches the free-surface, it flows radially towards the outside of the tank and then downwards near the outside wall and the circulation path is established. The tank gradually heats up and warm water starts accumulating at the top resulting in thermal stratification inside the tank. Progressively, the extent of the warmer region and stratification increase with time. An example of the temperature and velocity fields inside the tank is provided in Figure 4. Vapour was generated but boiling at the wall was observed to be minimal and, at least for the length of transients of the order of the one simulated, the large majority of vapour can be expected to be condensed in the subcooled liquid without reaching the free surface.

A preliminary comparison with the experimental measurements is provided in Figure 5. Figure 5(a) shows the axial distribution of the temperature very close to the heated wall. Except for regions close to the lower and upper surfaces, the agreement, although not totally accurate, is reasonable. In the lower region of the tank, the water is predicted to be much cooler than in the experiment, whereas it is warmer

close to the free-surface. This excessive stratification can be attributed to the inaccuracies of the turbulent heat flux modelling, which is currently limited to a simple extension of the eddy-viscosity concept (Eq. (8)) in the two-phase model. Radial profiles of the vertical mean velocity U_z are presented in Figure 5(b) at two different heights: $z / H = 0.9$ (close to the free surface) and 0.5 (in the middle of the tank). Except for the slight over prediction of the peak near the wall, the velocity profiles are in good agreement. Similarly to the square cavity, the majority of the flow is restricted to a very thin boundary layer region near the heated wall, whereas the recirculation velocity is much lower in the remainder of the water tank.

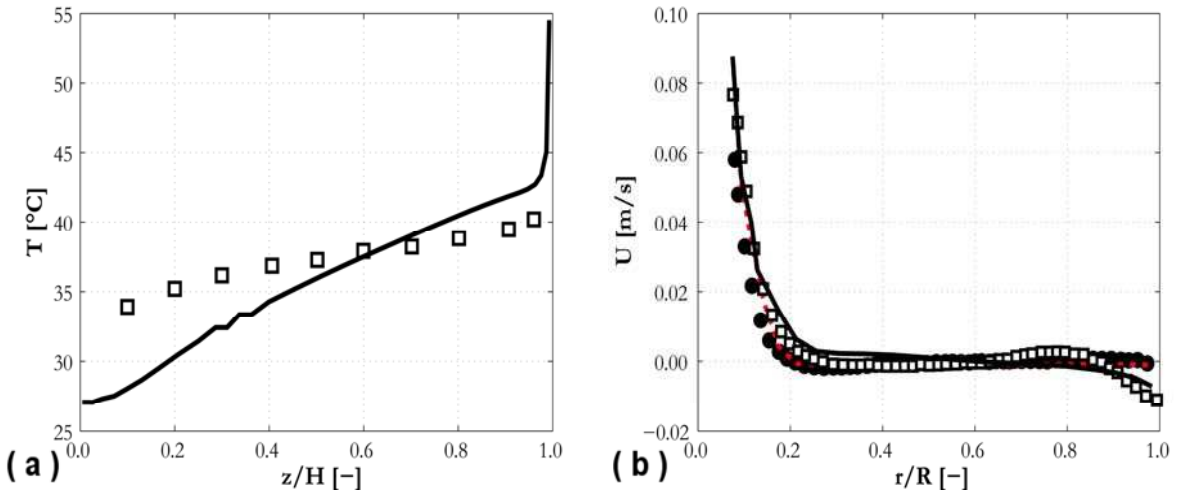


Figure 5. Profiles of liquid temperature (a) and water velocity (b) compared against experiments. (a) axial profile at $r / R = 0.087$. (b) radial profiles at: (□, —) $z / H = 0.9$; (●, ---) $z / H = 0.5$.

5. CONCLUSIONS AND FUTURE WORK

Activities ongoing at the University of Leeds towards the development of a CFD model, implemented in STAR-CCM+, for the prediction of buoyancy-driven flows and the thermal load during ERVC, including boiling at the wall, were presented in the paper. In natural convection, strong interactions occur between the turbulence and buoyancy force fields. A single-phase CFD model, based on a low-Reynolds number turbulence formulation, was tested against experiments in a square buoyant cavity and modifications were introduced to an algebraic formulation of the turbulent heat fluxes. Although agreement was improved and average flow quantities were well predicted, the model is still unable to correctly predict the structure of the turbulent heat transfer. Improvements are expected from the upgrade of the turbulence model to a Reynolds stress formulation, which will be implemented in the near future, which is expected to benefit much more from the application of an advanced model of the turbulent heat flux [6]. This will also be supported by the availability of detailed LES results from a model that, although still requiring improvement and analysis on the sub-grid contributions, was demonstrated to be superior to RANS approaches when applied to the same square buoyant cavity.

A two-fluid Eulerian-Eulerian boiling model, which will be required to predict ERVC, was also preliminary tested against an experiment for natural convection in a cylindrical tank with a vertical heated rod in the middle. The model was shown to behave reasonably well, providing quite good predictions of the velocity field in the tank. Additional testing is required to assess the capability of the model to predict thermal stratification and boiling at the wall, since only a very low generation of vapour was observed in the experiment considered. Standard models for turbulence and wall boiling are included at the present time that may limit the overall accuracy. In the future, turbulence prediction will be improved by

including advances made from the single-phase studies, and the wall boiling model will be developed using results from a parallel activity [32] on the CFD simulation of forced convection boiling. The whole model will then be assessed against the tests for ERVC in a scaled calandria vessel of the Indian pressure-tube type reactor performed at the Bhabha Atomic Research Centre (BARC) in Mumbai, India, in the framework of the UK-India Civil Nuclear Collaboration.

ACKNOWLEDGMENTS

The authors gratefully acknowledge the financial support of the EPSRC under grant EP/M018733/1, Grace Time, part of the UK-India Civil Nuclear Collaboration.

REFERENCES

1. IAEA, “Passive safety systems and natural circulation in water cooled nuclear power plants”, *IAEA-TECDOC-1624*, Vienna, Austria (2009).
2. S.H. Chang, S.H. Kim and J.Y. Choi, “Design of integrated passive safety system (IPSS) for ultimate passive safety of nuclear power plants”, *Nuclear Engineering and Design*, **260**, pp.104-120 (2013).
3. D.N. Basu, S. Bhattacharyya and P.K. Das, “A review of modern advances in analyses and applications of single-phase natural circulation loop in nuclear thermal hydraulics”, *Nuclear Engineering and Design*, **280**, pp. 326-348 (2014).
4. N. Minocha, J.B. Joshi, A.K. Nayak and P.K. Vijayan, “3D CFD simulations to study the effect of inclination of condenser tube on natural convection and thermal stratification in a passive decay heat removal system”, *Nuclear Engineering and Design*, **305**, pp. 582-603 (2016).
5. K. Hanjalic, “One-point closure models for buoyancy-driven turbulent flows”, *Annual Review of Fluid Mechanics*, **34**, pp. 321-347 (2002).
6. S.K. Choi and S.O. Kim, “Turbulence modeling of natural convection in enclosures: A review”, *Journal of Mechanical Science and Technology*, **26**, pp. 283-297 (2012).
7. A. Omranian, T.J. Craft and H. Iacovides, “The computation of buoyant flows in differentially heated inclined cavities”, *International Journal of Heat and Mass Transfer*, **77**, pp. 1-16 (2014).
8. T.I. Kim, H.M. Park and S.H. Chang, “CHF experiments using a 2-D curved test section with additives for IVR-ERVC”, *Nuclear Engineering and Design*, **243**, pp. 272-278 (2012).
9. J.J. Rempe, K.Y. Suh, F.B. Cheung and S.B. Kim, “In-vessel retention of molten corium: lessons learned and outstanding issues”, *Nuclear Technology*, **161**, pp. 210-267 (2008).
10. S. Rouge, “SULTAN test-facility for large-scale vessel coolability in natural convection at low pressure”, *Nuclear Engineering and Design*, **169**, pp.185-195 (1997).
11. Y.H. Jeong and S.H. Chang, “Critical heat flux experiments on the reactor vessel wall using 2-d slice test section”, *Nuclear Technology*, **152**, pp. 162-169 (2004).
12. E. Krepper, E.F. Hicken and H. Jaegers, “Investigation of natural convection in large pools”, *International Journal of Heat and Fluid Flow*, **23**, pp. 359-365 (2002).
13. M.S. Gandhi, J.B. Joshi and P.K. Vijayan, “Study of two-phase thermal stratification in cylindrical vessels: CFD simulations and PIV measurements”, *Chemical Engineering Science*, **98**, pp. 125-151 (2013).
14. M.S. Gandhi, J.B. Joshi, A.K. Nayak and P.K. Vijayan, “Reduction in thermal stratification in two-phase natural convection in rectangular tanks: CFD simulations and PIV measurements”, *Chemical Engineering Science*, **100**, pp. 300-325 (2013).
15. CD-adapco, *STAR-CCM+® Version 10.04 User Guide* (2015).
16. F. Ampofo and T.G. Karayannidis, “Experimental benchmark data for turbulent natural convection in an air filled square cavity”, *International Journal of Heat and Mass Transfer*, **46**, pp. 3551-3572 (2003).
17. D.G. Barhangi and L. Davidson, “Natural convection boundary layer in a 5:1 cavity”, *Physics of Fluids*, **19**, 125106 (2007).

18. D. Ammour, T. Craft and H. Iacovides, "Highly resolved LES and URANS of turbulent buoyancy-driven flow within inclined differentially-heated enclosures", *Flow, Turbulence and Combustion*, **91**, pp. 669-696 (2013).
19. R. Kumar and A. Dewan, "A study of LES-SGS closure models applied to a square buoyant cavity", *International Journal of Heat and Mass Transfer*, **98**, pp. 164-175 (2016).
20. H.G. Weller, G. Tabor, H. Jasak and C. Fureby, "A tensorial approach to computational continuum mechanics using object-oriented techniques", *Computers in Physics*, **12**, pp. 620-631 (1998).
21. W.P. Jones and B.E. Launder, "The prediction of laminarization with a two-equation model of turbulence", *International Journal of Heat and Mass Transfer*, **15**, pp. 301-314 (1972).
22. W. Xu, Q. Chen and F.T.M. Nieuwstadt, "A new turbulence model for near-wall natural convection", *International Journal of Heat and Mass Transfer*, **41**, pp. 3161-3176 (1998).
23. F.S. Lien, W.L. Chen and M.A. Leschziner, "Low-Reynolds number eddy-viscosity modelling based on non-linear stress-strain/vorticity relations", *Proceedings of the 3rd Symposium on Engineering Turbulence Modelling and Measurements*, Crete, Greece, May 27-29, 1996.
24. S. Kenjeres, S.B. Gunarjo and K. Hanjalic, "Contribution to elliptic relaxation modelling of turbulent natural and mixed convection", *International Journal of Heat and Fluid Flow*, **26**, pp. 569-586.
25. A. Yoshizawa, "Statistical theory for compressible turbulent shear flows, with the application to subgrid modelling", *Physics of Fluids*, **29**, pp. 2152-2164 (1986).
26. N. Kurul and M.Z. Podowski, "Multidimensional effects in forced convection subcooled boiling", *9th International Heat Transfer Conference*, Jerusalem, Israel, 1990.
27. T. Hibiki and M. Ishii, "Active nucleation site density in boiling systems", *International Journal of Heat and Mass Transfer*, **46**, pp. 2587-2601 (2003).
28. G. Kocamustafaogullari, "Pressure dependence of bubble departure diameter for water", *International Communications in Heat and Mass Transfer*, **10**, pp. 501-509 (1983).
29. R. Cole, "A photographic study of pool boiling in the region of the critical heat flux", *AICHE Journal*, **6**, pp. 533-538 (1960).
30. W.E. Ranz and W.M. Marshall, "Evaporation from drops", *Chemical Engineering Progress*, **48**, pp. 141-146 (1952).
31. S. Kenjeres and K. Hanjalic, "Prediction of turbulent thermal convection in concentric and eccentric horizontal annuli", *International Journal of Heat and Fluid Flow*, **16**, pp. 429-439 (1995).
32. M. Colombo and M. Fairweather, "Accuracy of Eulerian-Eulerian, two-fluid CFD boiling models of subcooled boiling flows", *International Journal of Heat and Mass Transfer*, **103**, pp. 28-44 (2016).